Supporting information

A Post-Synthetic Route for Modifying the Metal—Insulator Transition of VO_2 by Interstitial Dopant Incorporation

Theodore E. G. Alivio,[a,b†] Diane G. Sellers,[a,b†] Hasti Asayesh-Ardakani,[c,d] Erick J. Braham,[a,b] Gregory A. Horrocks,[a,b] Kate E. Pelcher,[a,b] Ruben Villareal,[b,e] Lucia Zuin,[f] Patrick J. Shamberger,[b] Raymundo Arróyave, [b,e] Reza Shahbazian-Yassar,[c,d] and Sarbajit Banerjee*[a,b]

[a] Department of Chemistry, Texas A&M University, College Station, Texas 77842-3012, United States

[b] Department of Materials Science and Engineering, Texas A&M University, College Station, Texas, 77843-3003, United States

[c] Department of Mechanical Engineering-Engineering Mechanics, Michigan Technological University, Houghton, Michigan 49933-1295, United States

[d] Department of Mechanical and Industrial Engineering, University of Illinois at Chicago, Chicago, Illinois 60607-7059, United States

[e] Department of Mechanical Engineering, Texas A&M University, College Station, Texas, 77843-3123, United States

[f] Canadian Light Source, University of Saskatchewan, Saskatoon S7N 2V3, Canada

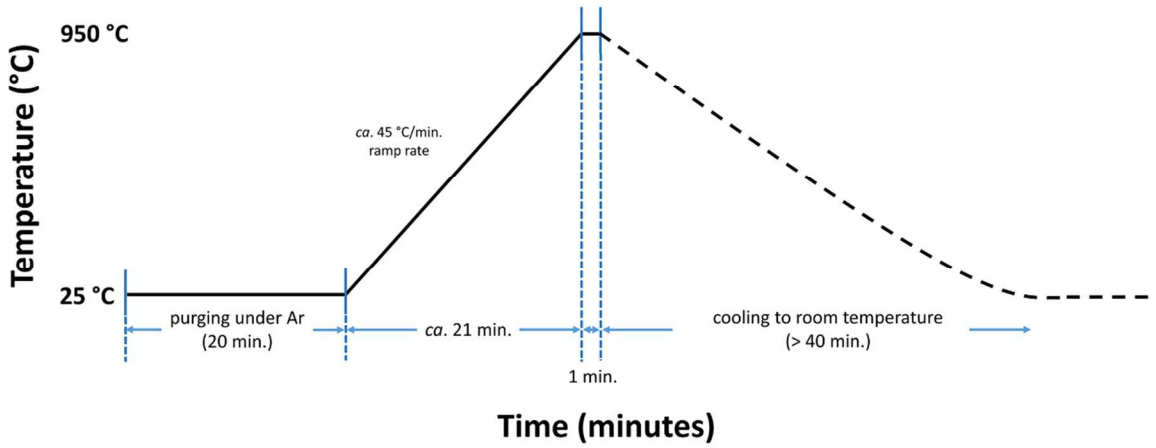

Figure S1: Rapid thermal annealing diagram for the diffusive doping process.

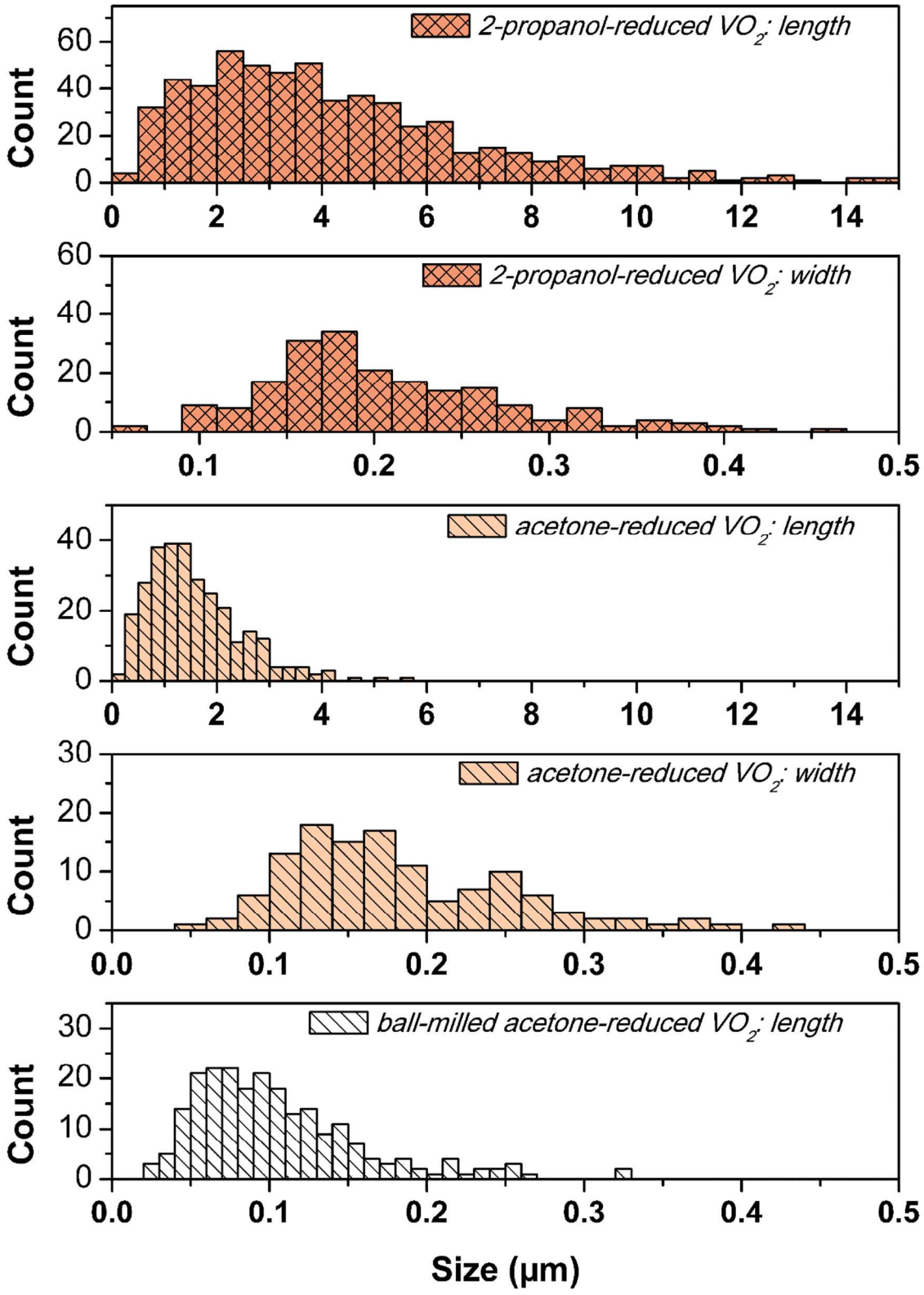

Figure S2: Size distribution histograms for VO_2 samples prepared by 2-propanol-reduction of V_2O_5, reduction of V_2O_5 by acetone, and reduction of V_2O_5 by acetone followed by ball milling. The dimensions are derived from TEM images.

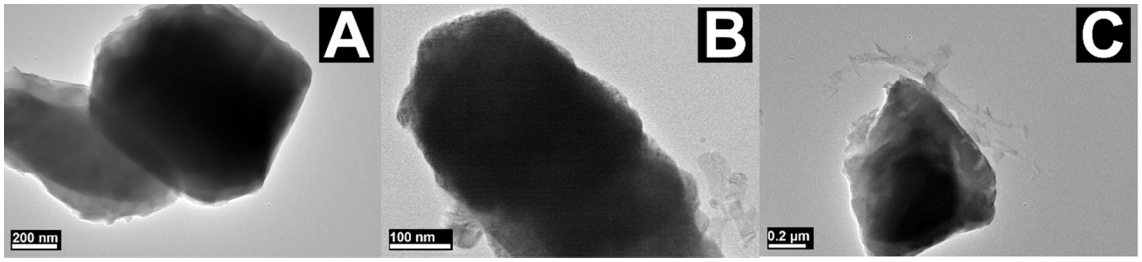

Figure S3: TEM images of B-incorporated samples of VO_2 nanowires reduced from A) 2-propanol, B) acetone, and C) acetone, subsequently ball-milled.

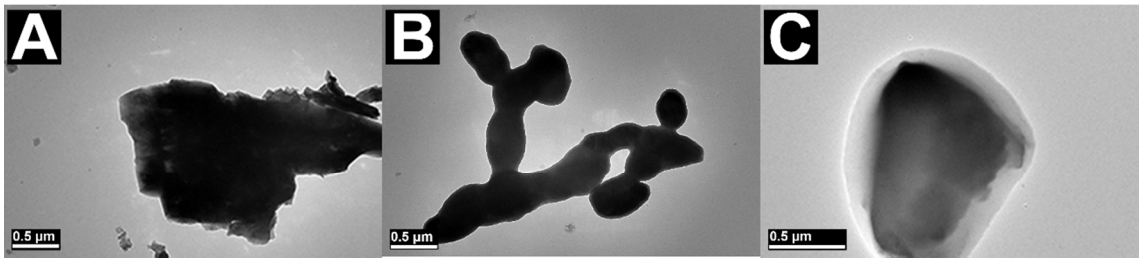

Figure S4: TEM images of VO_2 nanowires reduced from A) 2-propanol, B) acetone, and C) acetone, subsequently ball-milled annealed without exposure to the molecular B precursor.

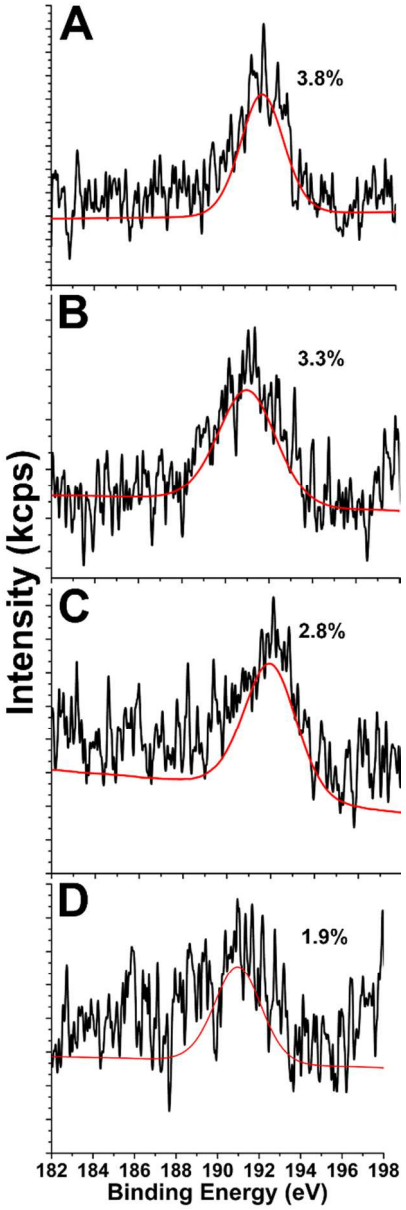

Figure S5: High-resolution B 1s XPS spectra of B-incorporated VO_2 samples with increasing B content. All fits (shown in red) are plotted as B-spline functions.

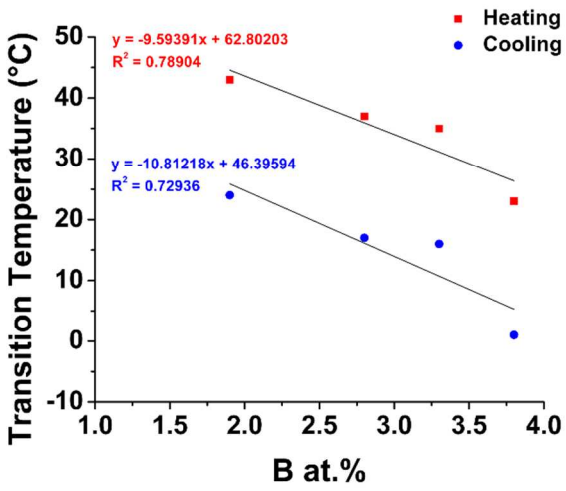

Figure S6: Linear relationship between atomic percent of B as deduced from XPS and VO_2 transition temperatures determined from DSC measurements.

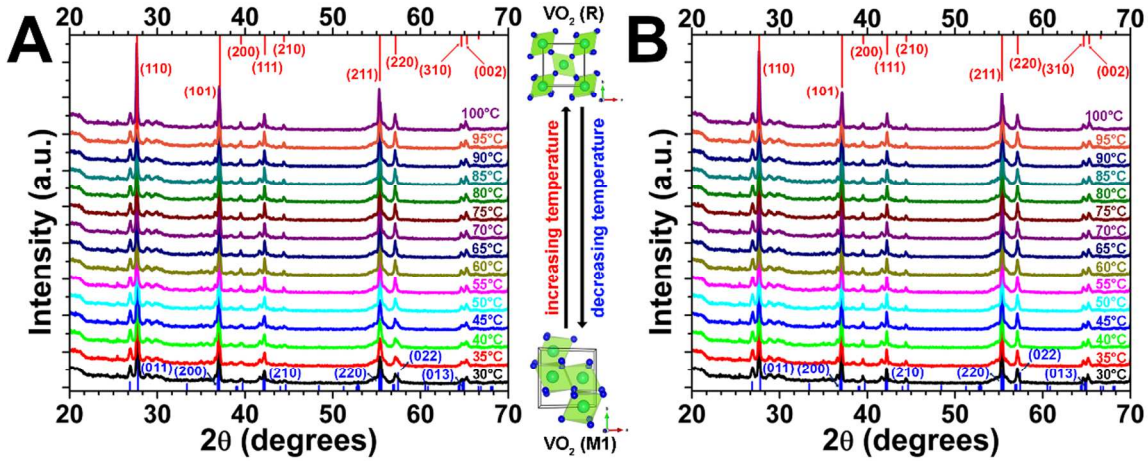

Figure S7: XRD patterns corresponding to *in situ* heating (a) and cooling (c) of a B-incorporated VO_2 sample collected at 5°C increments from 30 to 100 °C. Vertical bars indicate positions and relative intensities of reflections derived from JCPDS XRD patterns. Reflections of $VO_2(M_1)$ are indicated in blue (JCPDS # 43-1051) and $VO_2(R)$ in red (JCPDS # 79-1655).

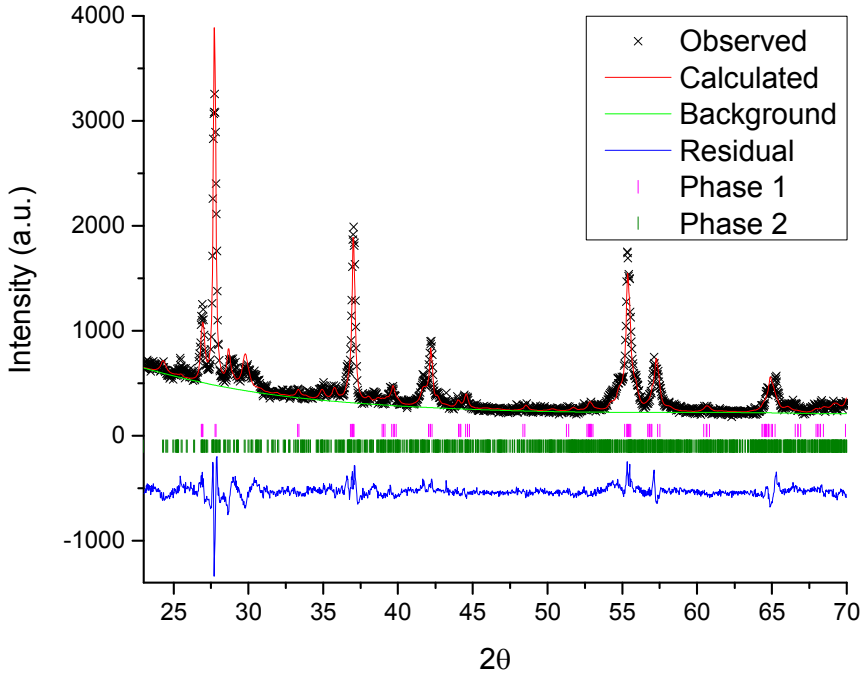

Figure S8. Rietveld refinement of powder XRD pattern of 2.8 at.% B-doped VO_2 nanocrystals acquired at 295 K (see Table S1 for details). Pink tick marks indicate the position of reflections corresponding to the P1 21/c 1 monoclinic space group of VO_2 whereas green tick marks indicate the position of reflections corresponding to the P -1 triclinic space group of V_8O_{15}.

Table S1.Tabulated parameters from a Rietveld refinement of 2.8 at.% B-doped VO_2 structure. Refinement statistics, including goodness of fit (χ^2), weighted goodness of fit (wRp) and the individual point residuals (Rp) show good agreement between the observed and calculated patterns.

Phase 1: $VO_2(M_1)$ // Space Group: P1 21/c 1 // Wt. Fraction: 0.55810 // Vol: 118.70(3) Å^3		
α = 90.000(0)°	β =122.31(2)°	γ= 90.000(0)°
a = 5.7424(8)	b = 4.539 (1)	c= 5.388(2)
X^2 = 4.511	wRp = 0.1040	Rp = 0.0834
Phase 2: V_8O_{15}(triclinic) // Space Group: P -1 // Wt. Fraction: 0.44190 // Vol: 916.095(0) Å^3		
α = 98.90(4)°	β = 128.46 (3)°	γ= 109.12(3)°
a = 5.450(3)	b = 7.011(2)	c= 37.04(1)
X^2 = 4.511	wRp = 0.1040	Rp = 0.0834

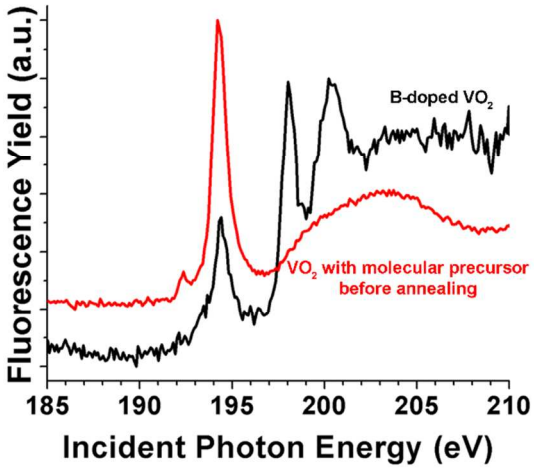

Figure S9: B K-edge XANES spectra of an acetone-reduced B-doped VO_2 sample before and after thermal annealing.

Table S2: Fractional atomic coordinates of viable interstitial and substitutional sites for B placement within a tetragonal VO_2 assessed using DFT calculations.

Site	x	y	z
I1	0.875000	0.000000	0.500000
I2	0.250001	0.411638	0.121699
I3	0.240321	0.875014	0.606839
V	0.500000	0.500000	0.250000
O	0.500000	0.779781	0.250000